Bull. Soc. géol. Fr., 2003, t. 174, n° 5, pp. 497-510

Geological boundary conditions of the 1909 Lambesc (Provence, France) earthquake : structure and evolution of the Trévaresse ridge anticline

DOMINIQUE CHARDON[1] and OLIVIER BELLIER[1]

Keywords. – SE France, Reverse faulting, Folding, Neogene-Quaternary, Seismotectonics.

Abstract. – The 06/11/1909, Lambesc, M=6 earthquake is the strongest instrumental seismic event recorded in French history. A review of the geology of the epicentral area combined with detailed field mapping and structural analysis allows constraining the tectonic and geomorphic evolution of the Trévaresse ridge anticline and associated fault that ruptured during the 1909 event.

The Trévaresse fold is a WNW-trending, southerly-verging forced ramp anticline developed above the Trévaresse reverse fault during late Miocene and Pliocene times, and possibly after the early Pleistocene. Over the last 11 Ma, the Trévaresse reverse fault records an average reverse slip rate of 0.03 ± 0.02 mm/yr consistent with a homogeneous N005 – N010 trending shortening direction. The fault is segmented into two major segments (the eastern one being linked to a possibly active frontal blind thrust fault) separated by a relay fault zone associated with an en-échelon fold pattern consistent with a slight left-lateral component on the easternmost segment. Our structural analysis combined with recent estimates of the source parameters of the Lambesc earthquake indicates that the fault has to reach at least the basement-cover interface, at a minimum depth of 6 km. The westward longitudinal decrease in morphological maturity of the relief of the Trévaresse ridge anticline and its associated fault scarp suggests a westward propagation of the fold during partly diachronous activation of the two segments of the fault.

Cadre géologique du séisme de Lambesc du 11 juin 1909 (Provence, France) : structure et évolution de l'anticlinal de la Trévaresse

Mots Clés. – Sud-Est de la France, Faille inverse, Plissement, Néogène-Quaternaire, Sismotectonique.

Résumé. – Le séisme de Lambesc du 11 juin 1909 (M = 6) est l'événement instrumental le plus important de l'histoire de France. L'analyse géologique de la zone épicentrale (synthèse, cartographie détaillée et étude tectonique) permet de contraindre l'évolution structurale et morphologique de l'anticlinal de la Trévaresse et de la faille associée ayant produit le séisme.

Le pli de la Trévaresse est un anticlinal de rampe "forcé" à vergence sud qui s'est développé sur la faille inverse de la Trévaresse du Miocène terminal au Pliocène et probablement après le Pleistocène inférieur. Au cours des 11 derniers millions d'années, la faille de la Trévaresse a enregistré un taux de déplacement inverse intégré de 0,03 ± 0,02 mm/an et un raccourcissement homogène orienté N005 – N010. La zone de faille est constituée de deux segments principaux (le segment oriental étant associé à une faille frontale aveugle potentiellement active) séparés par un relais associé à une série de plis en échelon compatible avec la faible composante senestre du segment oriental. La combinaison de l'analyse structurale avec les réestimations récentes des paramètres de source du séisme indique que la faille de la Trévaresse doit s'enraciner à une profondeur minimale de 6 km, c'est à dire au niveau de décollement triasique. La décroissance vers l'ouest de la maturité morphologique du chaînon anticlinal et de l'escarpement de faille associé suggère une propagation du pli vers l'ouest lors de l'activation partiellement diachrone des deux segments de la faille.

INTRODUCTION

The Lambesc earthquake (1909, June, 11th, M=6) is the most important seismic event that occurred in France during the last century. The earthquake took place in Provence (SE France), a region located at the junction of the Pyrenean and Alpine orogenic belts (fig. 1), that is undergoing overall N-S plate convergence. The example of the 1909 Lambesc event shows that despite its slow deformation rate and low instrumental seismicity, Provence may experience magnitude 6 earthquakes with long recurrence intervals. In addition, as the region undergoes significant erosion rates due to its Mediterranean climate and anthropic activity, seismic hazard assessment in Provence is particularly difficult [e.g., Peulvast *et al.*, 1999].

As no surface rupture was documented in the epicentral area [Spiess, 1926, and references therein] the identification of the fault that ruptured in 1909 was not straightforward. Reevaluations of the microseismic and seismological data

[1] Centre Européen de Recherche et d'Enseignement de Géosciences de l'Environnement (UMR CNRS 6635), Université Aix-Marseille 3, BP 80, F-13545 Aix-en-Provence cedex 4, France. Chardon@cerege.fr; Bellier@cerege.fr
Manuscrit déposé le 1er avril 2003 ; accepté après révision le 22 mai 2003.

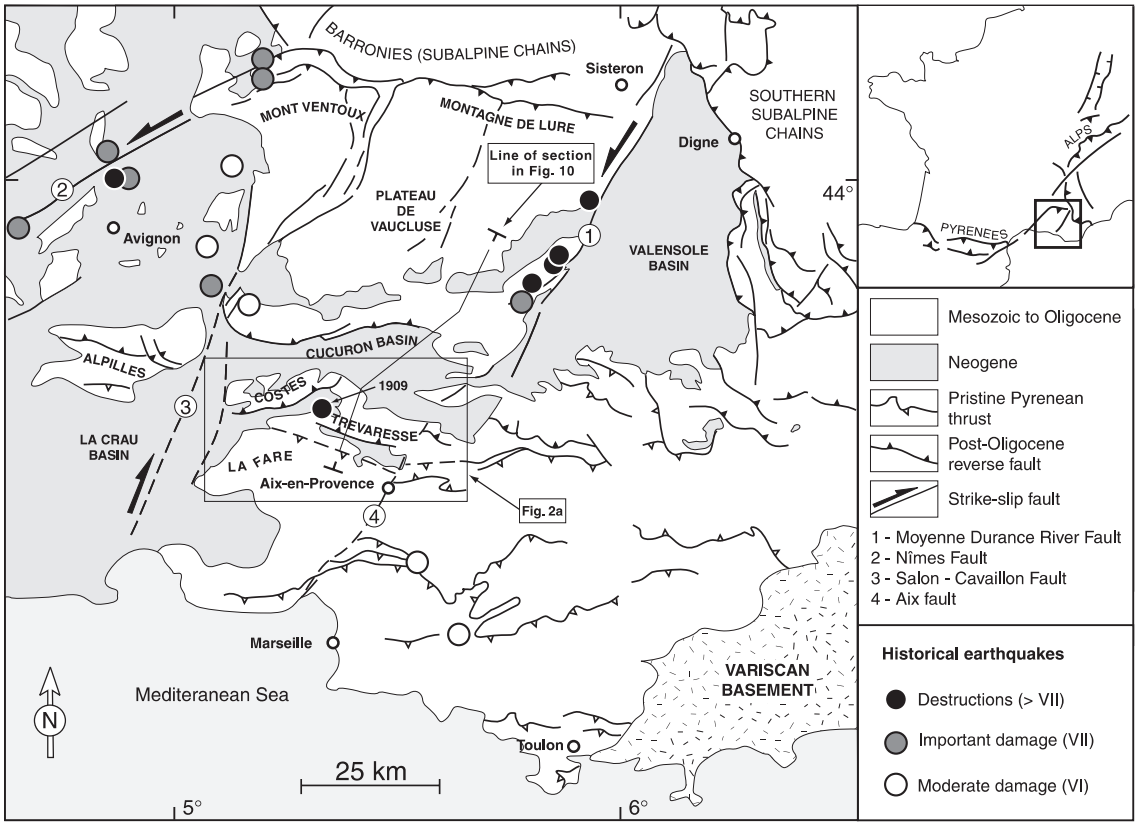

FIG. 1. – Structural map of western Provence adapted from Ritz [1991] and Terrier [1991], showing the epicenters of the main historical earthquakes (adapted from Lambert [1997]). The 1909 Lambesc earthquake epicenter [after Levret *et al.*, 1996] is shown. Faults 1, 2 and 4, together with the Mont Ventoux-Montagne de Lure thrust system, define the western Provence crustal panel.
FIG. 1. – *Schémas structural de la Provence occidentale d'après Ritz [1991] et Terrier [1991], montrant les épicentres des principaux séismes historiques (adaptés de Lambert [1997]). L'épicentre du séisme de Lambesc [d'après Levret* et al.*, 1996] est localisé. Les failles* 1, 2 *et* 4, *ainsi que les chevauchements du mont Ventoux et de la montagne de Lure délimitent le panneau ouest-provençal.*

indicate that the earthquake occurred on a fault underlying the Trévaresse ridge, a WNW trending anticline located to the SE of Lambesc [e.g., Levret *et al.*, 1986 ; Baroux *et al.*, 2001a ; 2002, 2003 ; Lacassin *et al.*, 2001] (fig. 1 and 2). The aim of the present contribution is to review the Neogene – Quaternary paleogeographic and structural frame of the Trévaresse ridge anticline in order to constrain its structure, kinematics and long-term morphotectonic evolution, and to present a reappraisal of its tectonic setting. This provides key boundary conditions for the 1909 earthquake and tests of the geometry of the fault that ruptured.

GEOLOGICAL AND SISMOTECTONIC REGIONAL BACKGROUND

Provence coincides with a late Cretaceous to Paleogene (i.e., Pyrenean), north-verging fold-and-thrust belt [Tempier, 1987] (fig. 1). So-called Pyrenean thrusts are preserved in southern Provence, whereas Pyrenean structures were reactivated in the north during Neogene shortening that led to dominantly south-verging thrust faults in West-Central Provence [e.g., Combes, 1984 ; Villeger and Andrieux, 1987] (fig. 1 and 2). Two NE-trending, crustal-scale sinistral strike-slip faults (the Nîmes and Moyenne Durance river faults, fig. 1) contributed to the partitioning of differential N-S shortening during the Pyrenean and Neogene shortening episodes. These faults coincide with the main clusters of historical earthquakes [Lambert, 1997] (fig. 1) and display evidence for Quaternary faulting revealed by paleoseismological [Combes *et al.*, 1993 ; Sébrier *et al.*, 1997 ; Dutour *et al.*, 2002] or structural [Hippolyte and Dumont, 2000] studies. Indices of Quaternary deformation were also reported from along the Salon – Cavaillon fault [Terrier, 1991 ; Vella and Provansal, 2000] and from the southern limb of the La Fare anticline [Gabert, 1965 ; Provansal *et al.*, 1995] (fig. 1). The 1909 earthquake attests to the seismic activity of the reverse fault system affecting the interior of the western Provence crustal panel [Combes, 1984] (fig. 1).

How the intraplate Provence domain currently behaves to accommodate the north-south plate convergence at an overall rate of 6 mm/yr [DeMets *et al.*, 1990] is a matter of debate. The N-S shortening rate of the region obtained by restoring the Miocene strata on a regional cross section of Provence is of the order of 0.1 mm/yr over the last 20 Ma [Champion *et al.*, 2000]. Similar values are obtained by estimating slip rates along the Moyenne Durance river and Nîmes faults based on the offset of Neogene stratigraphic markers, Plio-Quaternary drainage networks or alluvial terraces [Peulvast *et al.*, 1999 ; Baroux, 2000 ; Hippolyte and Dumont, 2000 ; Schlupp *et al.*, 2001]. Geodetic work by Ferhat *et al.* [1998] suggested that the cumulated

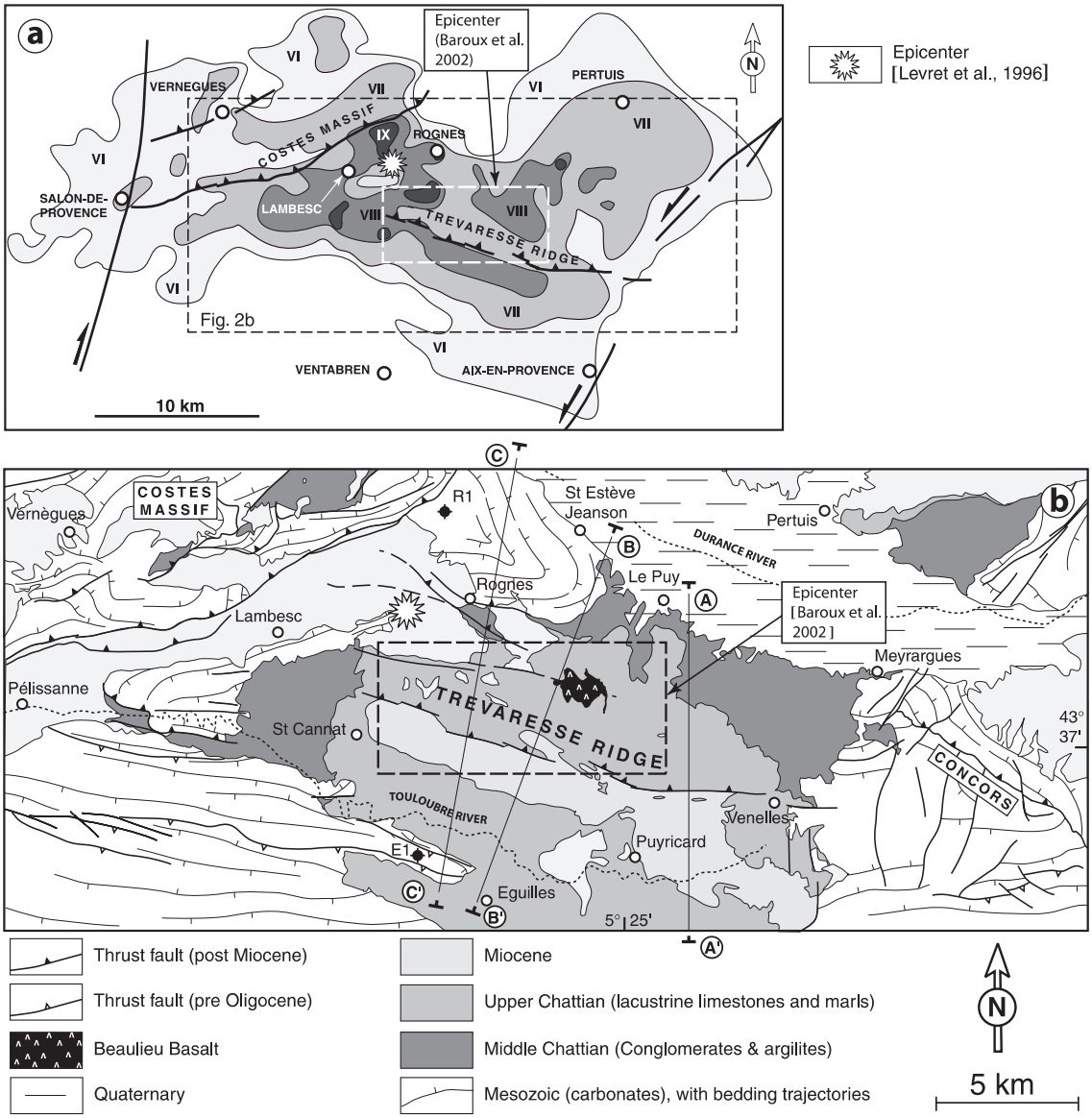

FIG. 2. – (a) Intensity map of the 1909 Lambesc earthquake (adapted from Lambert [1997]), located on figure 1. (b) Simplified geology of the epicentral area of the 1909 Provence earthquake. After Dubois, [1964] ; Busser and Pachoud [1966] ; Gouvernet *et al.* [1968, 1970] and the present work. E1, R1 : drill holls *Eguilles 1* and *Rognes 1*, respectively (see fig. 3c).
FIG. 2. – (a) *Carte des intensités du séisme de Lambesc (adapté de Lambert, [1997]), localisée sur la figure 1.* (b) *Géologie simplifiée de la zone épicentrale. D'après Dubois, [1964] ; Busser et Pachoud [1966] ; Gouvernet* et al. *[1968, 1970] et la présente étude.* E1 *et* R1 *sont les forages Eguilles 1 and Rognes 1 (voir fig. 3c).*

transcurrent slip rate on both the Moyenne Durance River and Nîmes faults cannot exceed 2 mm/yr [see also Jouanne *et al.*, 2001]. Recent permanent Global Positioning System (GPS) measurements [Calais *et al.*, 2002] indicate NW-directed compression over the southern part of the western Alps and Provence at a strain rate of 0.01 μ strain/yr. From a kinematic point of view, this result agrees with the earthquake focal mechanism analyses around the Moyenne Durance River Fault [Volant *et al.* ; 2000 ; Baroux *et al.*, 2001b]. However, Baroux *et al.* [2001b] suggest two distinct, seismically determined stress fields within the western Provence panel. Indeed, their results indicate active E-W extension in the Rhône river valley area, west of the Salon-Cavaillon fault (fig. 1).

THE LAMBESC (1909, JUNE, 11TH) EARTHQUAKE

The event produced maximum MSK intensities of IX [Spiess, 1926, and references therein ; Levret *et al.*, 1986, 1996 ; Lambert, 1997] (fig. 2a) and magnitudes of $M_w = 6$, $M_s = 6$ and $M_e = 5.8$ (for the most recent estimates by Baroux *et al.* [2002, and 2003]). It caused 46 fatalities and about 305 million euros of damages [reassessment for 1982 by the French Ministry of Environment]. It was felt over an area of about 100,000 km^2, intensities III reaching Italy and Spain. The VIII isoseismal is elongate in the WNW direction, parallel to the Trévaresse ridge [Levret *et al.*, 1996 ; Lambert, 1997 ; Baroux *et al.*, 2001a ; 2002 ; Lacassin *et al.*, 2001] (fig. 2a). The epicenter locations deduced from

intensity data, by excluding site effect locality data at Rognes and Vernègues (fig. 2a) [Levret *et al.*, 1996 ; Baroux *et al.*, 2002, 2003], are located between the traces of the Trévaresse and Rognes faults (fig. 2b). Furthermore, reprocessing of the available seismograms by Baroux *et al.* [2003] suggests a rupture along a N-110 trending, steeply north dipping reverse fault with a slight dextral component. Given its strike and dip direction, the Trévaresse fault therefore appears as the only candidate to have ruptured in 1909.

The coseismic vertical displacement field deduced from topographic leveling data of Lallemand [1911] by Romieu *et al.* [1998] shows 12 cm of N-S, relative regional differential north-side up (or south-side down) movement across the epicentral area between Pertuis and Ventabren (fig. 2). Baroux *et al.* [2003] used their seismologically constrained model fault to predict the elevation change due to the 1909 event by running an elastic dislocation model. Their simulation is compatible with the coseismic elevation changes of Lallemand [1911] re-evaluated by Romieu *et al.* [1998] in the vicinity of the Trévaresse ridge.

STRUCTURE AND KINEMATICS OF THE TRÉVARESSE RIDGE ANTICLINE

Geological outline of the epicentral area

The Trévaresse ridge is the morphological expression of an anticline located within the Aix-en-Provence Oligocene Basin, a half-graben developed against the Aix-en-Provence fault [Nury, 1990] that is partly sealed by Chattian deposits between Meyrargues and Aix-en-Provence (fig. 1 and 2). The floor of the half graben was tilted towards the ESE during W-side-down normal faulting along the Aix Fault [Hippolyte *et al.*, 1993], resulting in an increasingly thick Chattian sedimentary cover from west to east (fig. 3). The Oligocene basin lies unconformably on the Mesozoic sediments folded and faulted during the Pyrenean deformation episode (fig. 2). This is especially exemplified by the North Provençal thrust, a major Pyrenean structure recognized in a drill hole near Eguilles (fig. 2 and 3c), that is sealed by the Chattian beds [Busser and Pachoud, 1966 ; Guieu and Rousset, 1978]. Pyrenean structures and Oligocene sediments are in turn unconformably overlain by the Cucuron Miocene foreland basin that is bounded to the north by the Luberon range [Aguilar and Clauzon, 1982 ; Clauzon and Robert, 1984 ; Clauzon, 1996] (fig. 1). South of the Durance River, the Miocene deposits of the Cucuron basin are deformed by the Costes, Rognes, Concors and Trévaresse folds [Gouvernet, 1963 ; Dubois, 1964, 1966 ; Combes, 1984 ; Carbon, 1996] (fig. 2b).

Structure

The Trévaresse ridge anticline refolds the synclinorium-shape Aix-en-Provence Oligocene basin (fig. 3). The fold is steeply inclined, horizontal. Its ~ 5-km-long back limb is

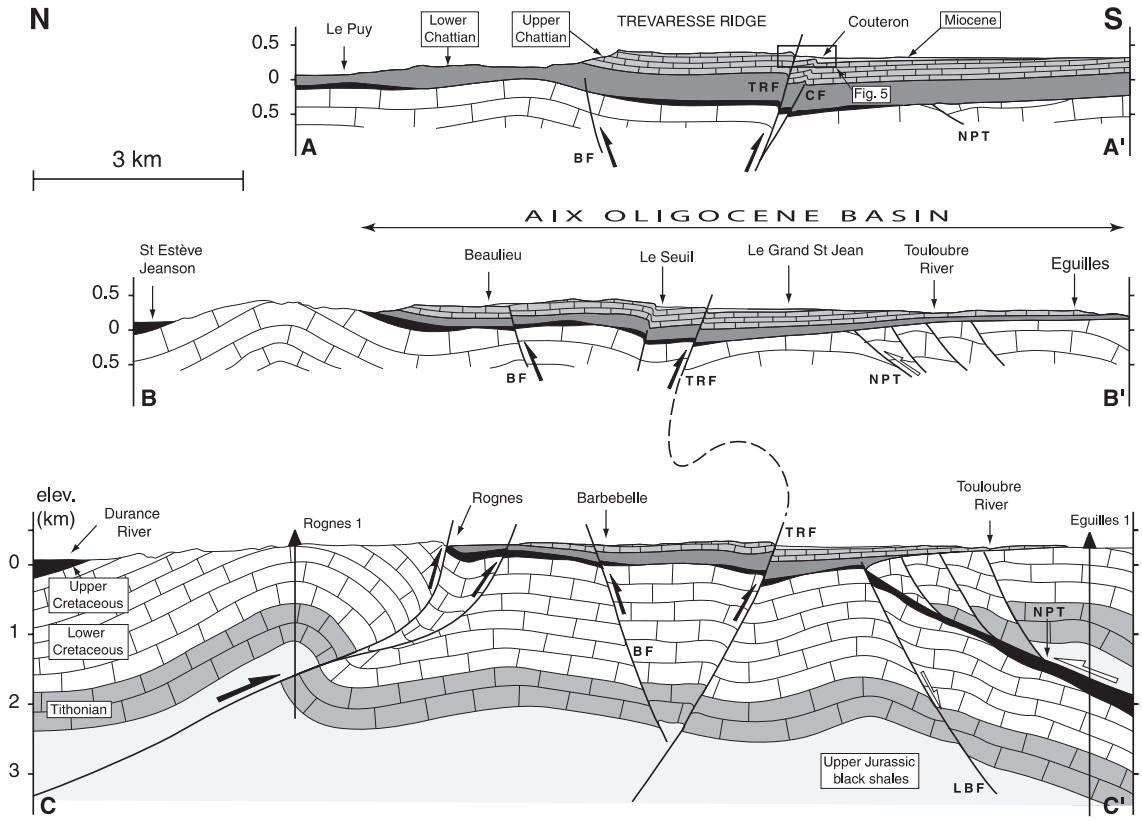

FIG. 3. – Serial cross-sections through the epicentral area of the 1909 Lambesc earthquake showing the Trévaresse ridge anticline and adjoining structures. The lines of section are located on figure 2b. Complementary sources : Busser and Pachoud [1966] ; Gouvernet *et al.* [1968, 1970] ; Guieu and Rousset [1978]. NPT – North Provençal Thrust ; TRF – Trévaresse Reverse fault ; BF – Beaulieu fault ; CF – Couteron blind reverse fault ; LBF – La Barben fault.
FIG. 3. – *Coupes sériées de la zone épicentrale montrant l'anticlinal de la Trévaresse et les structures avoisinantes (localisation sur la figure 2b). Sources complémentaires : Busser et Pachoud [1966] ; Gouvernet* et al. *[1968, 1970] ; Guieu et Rousset [1978].* NPT – *chevauchement Nord Provençal ;* TRF – *faille de la Trévaresse ;* BF – *faille de Beaulieu ;* CF – *faille aveugle de Couteron ;* LBF – *faille de La Barben.*

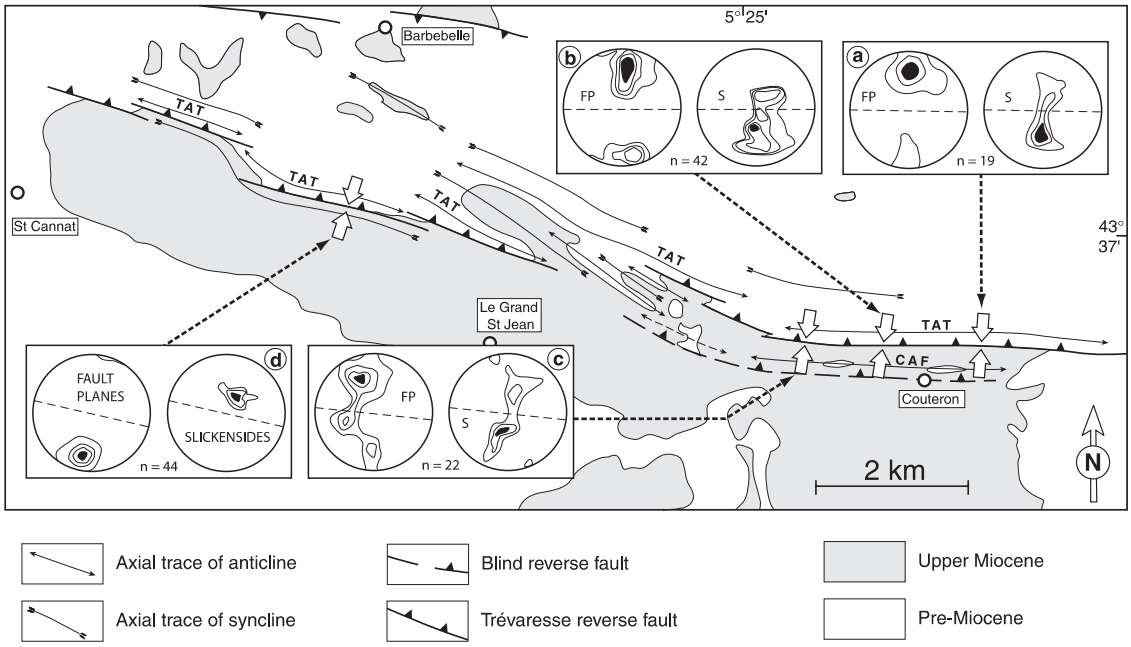

FIG. 4. – Detailed structural map of the Trévaresse reverse fault. Lower hemisphere, equal area stereograms of microtectonic data (poles to fault planes and slickensides) are shown. The white arrows indicate the maximum shortening axes deduced from the fault populations (see figure 6 for details). Dashed lines on stereograms represent the strike of the fault trace. Stations (a) and (b) are located in Chattian limestones from the hanging-wall of the fault. Station (c) is located within the late Tortonian conglomerates from the footwall of the fault. Station (d) is located within the main fault gauge affecting Chattian limestones and Serravallian molasses. TAT – Trévaresse ridge anticline axial trace ; CAT – Couteron anticline axial trace.
FIG. 4. – *Carte structurale détaillée de la faille de la Trévaresse montrant les données microtectoniques (fractures et stries). Les flèches blanches représentent les directions de raccourcissement maximum déduites de l'inversion des populations de failles (détails sur la figure 6). Les lignes pointillées représentent la direction de la trace de la faille. Les stations* (a) *et* (b) *sont situées dans les calcaires chattiens de l'anticlinal de la Trévaresse. La station* (c) *est située dans les conglomérats Valensole I du synclinal de Puyricard. La station* (d) *est située dans la gouge de faille affectant la molasse serravallienne et les calcaires chattiens de la Trévaresse.* TAT – *trace axiale de l'anticlinal de la Trévaresse ;* CAT – *trace axiale de l'anticlinal de Couteron.*

homoclinal and sub horizontal to gently N-dipping. Its forelimb is very short (less than 200-m-long), sub vertical to gently reclined and sheared against the Trévaresse reverse fault (called hereafter TRF) that dips 60 to 80° to the north. In the eastern and central parts of the ridge (fig. 3a and 3b), the back limb of the fold is affected by the eastern termination of the Rognes anticline (fig. 2b). In the western part of the ridge, the back limb of the Trévaresse fold is cut by the fault ramp that underlies the Rognes anticline (fig. 3c).

The forelimb and hinge line of the anticline trend parallel to the TRF and the hinge line is systematically very close (20 m) to the fault. With such a low curvature radius, the fold is interpreted as a short wavelength kink-band accompanying drag folding against the TRF (fig. 4 and 5). Detail field mapping combined with aerial photograph and SPOT images interpretation allows identifying two main segments for the TRF, that in turn consist in several secondary segments (fig. 4). The E-trending segment is mapped from Venelles westward and bents into WNW strikes close to its western termination. The western segment starts NE of Le Grand St Jean, stretches up to St Cannat and trends N 112 E. The main Trévaresse fold hinge is segmented consistently with the fault segmentation, leading to a non-cylindrical geometry for the fold (fig. 4). The gap between the two fault segments (~ 600 m across-strike and ~ 800 m along-strike) displays a series of folds with axial surfaces trending parallel to the western termination of the eastern fault segment (fig. 3b and 4). Those folds correspond to digitations of the Puyricard syncline (fig. 2) that flanks the Trévaresse ridge anticline to the south. This fold is symmetrical to the anticline with respect to the TRF, with a gently north-dipping homoclinal southern limb and a short, vertical to gently reclined northern limb (fig. 2 and 3). At the front of the eastern TRF segment and north of Couteron, the southern limb of the syncline is refolded into a short-wavelength, steeply inclined, horizontal anticline, called hereafter the Couteron anticline (fig. 3a, 4 and 5a). The very short curvature radius of this anticline, similar to the main Trévaresse ridge anticline, suggests that the fold is associated with a blind reverse fault (i.e., the Couteron blind reverse fault ; fig. 3a and 5a) that is interpreted to root into the eastern segment of the TRF.

In the western part of the Trévaresse ridge, the back limb of the anticline is affected by an E-W trending, steeply S-dipping reverse fault mapped between Lambesc and the Beaulieu volcanic complex (called hereafter the Beaulieu fault ; fig. 2 and 3). The orientation and kinematics of this structure confers a pop-up geometry to the western Trévaresse ridge (fig. 3c) that cuts across the back limb of the anticline.

Trevaresse reverse fault kinematics

The present work has allowed reassessing the surface trace pattern of the TRF that had previously been reported on geological maps [Gouvernet *et al.*, 1968, 1970]. This interpretation of a southerly-verging reverse fault at the forelimb of the Trévaresse ridge anticline was originally suggested

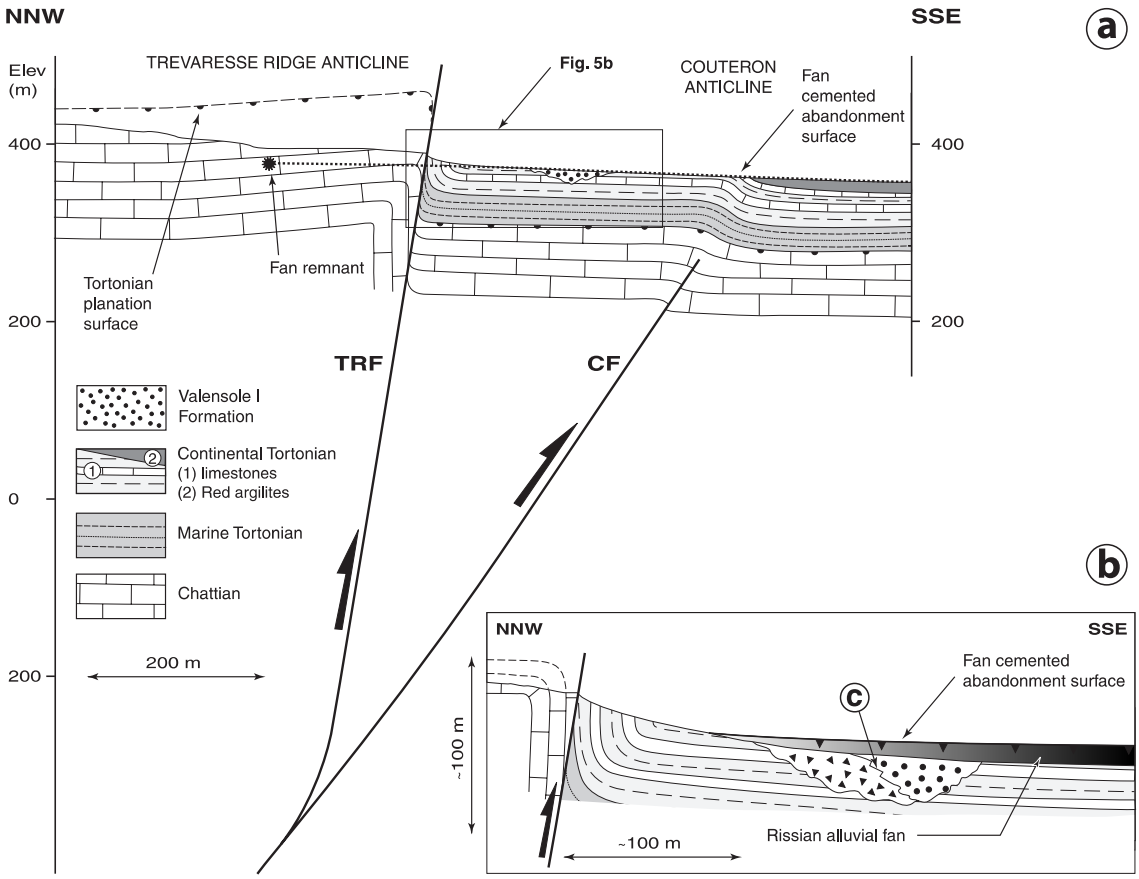

FIG. 5. – (a) Cross-section of the forelimb of the Trévaresse ridge anticline showing its relations with the Couteron anticline (located on figure 3a and 7, at station c). (b) Large-scale schematic section of the transition between the Trévaresse ridge and its piedmont at the same location (located on fig. 7a). Location of microtectonic station (c) (figure 4 and 7) is shown.
FIG. 5. – (a) *Coupe du flanc sud de l'anticline de la Trévaresse et de l'anticlinal de Couteron (localisation station* (c)*, figure 4 et 7).* (b) *Coupe schématique du détail de la transition entre le massif de la Trévaresse et son piemont (localisé sur la figure 5a). La station microtectonique* (c) *est localisée sur la coupe.*

by Dubois [1964] (cross-sections), for some segments of the fold, and partly documented by reconnaissance structural studies [Combes, 1984 ; Carbon, 1996 ; Champion *et al.*, 2000]. In their reconnaissance geomorphic study of the Trévaresse ridge, Lacassin *et al.* [2001] suggested the same interpretation of a reverse fault bounding the Trévaresse ridge anticline that was however challenged by Mattauer [2002] who advocated the lack of evidence for faulting at the surface. In their response, Lacassin *et al.* [2002] proposed a detailed cross-section of the easternmost part of the eastern TRF segment similar to the one drawn by Carbon [1996], that convincingly argues for an emerging reverse fault zone along the forelimb of the Trévaresse ridge anticline.

Structural relations are consistent all along the TRF. Chattian limestones and Miocene beds are concordant and the Miocene series are often attenuated (fig. 5a). For instance, at station (d) (fig. 4), calcareous molasses are turned into a fault gauge of several meters width, displaying pervasive, bed-parallel, dip-slip reverse shearing (fig. 6d). North-side up kinematics are also attested to by the angular relationships between bedding and schistosity observed in recent excavations along the eastern segment of the fault (fig. 1b *in* Lacassin *et al.* [2002]). Those relations are not consistent with flexural slip folding of the anticline. They require reverse faulting to have taken place at the forelimb of the fold and confirm that the TRF reaches the surface and has contributed to north-side up movement.

We performed a quantitative inversion of fault slip data measured at four sites (fig. 4) along the TRF using the method originally proposed by Carey [1979] [e.g., Mercier *et al.*, 1991]. Along the eastern segment of the fault, the great circles bearing the poles to the fault planes and slickensides do not trend perpendicular to the trace of the fault (fig. 4), suggesting a slight clockwise obliquity between outcrop – scale fractures and the main fault (fig. 4). This is confirmed by the inversion results (fig. 6) that indicate 4 to 6° of clockwise deviation of the shortening principal stress direction with respect to the normal to the fault trace (fig. 4). These results therefore suggest a dominantly dip-slip with a minor sinistral component on the eastern TRF segment. Relative chronology arguments within the fault population at station (b) provide evidence for two distinct reverse faulting episodes (fig. 6). Early striae reflect a slight dextral component with respect to the TRF, whereas later ones are compatible with a sinistral component. As this observation is local, it is interpreted to result from superimposed slip directions during fold amplification and/or reverse faulting histories. In spite of this exception, no variation in paleokinematics is documented. One should add

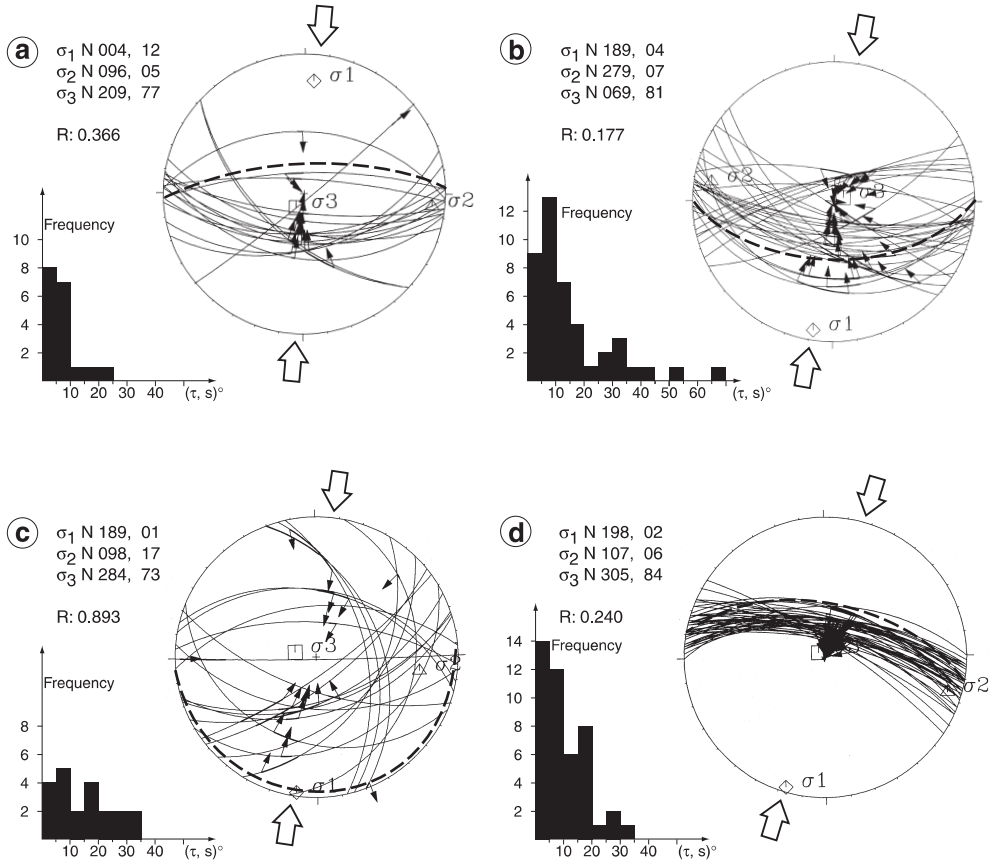

FIG. 6. – Results of the fault-slip data inversion along the Trévaresse reverse fault. Stations are shown on figure 4. Thick dashed lines indicate the average bedding plane. Histograms show the deviation between the striation (**s**) and the resolved shear stress (τ) for each fault plane. R is a stress ratio parameter defined as $R = (\sigma_2 - \sigma_3)/(\sigma_3 - \sigma_1)$, the σ_1, σ_2 and σ_3 axes corresponding to the maximum, intermediate and minimum principal stress axes, respectively.
FIG. 6. – *Résultats des inversions de populations de faille le long de la faille de la Trévaresse. Les stations sont localisées sur la figure 4. Le plan moyen de stratification est figuré par une ligne tiretée. Les histogrammes montrent l'écart angulaire entre la strie mesurée (**s**) et la contrainte tangentielle calculée* (τ) *pour chaque plan de faille.* R *est défini par* $R = (\sigma_2 - \sigma_3)/(\sigma_3 - \sigma_1)$, σ_1, σ_2 *et* σ_3 *étant les contraintes principales.*

that kinematics are particularly well constrained as attested to by the consistency between inversion results obtained in Chattian limestones and late Tortonian conglomerates (fig. 6).

Along the western TRF segment (station d, fig. 4 and 6), the fracture planes trend systematically parallel to the fault trace and the slickensides have a down-dip orientation (fig. 6d). This indicates that the outcrop-scale fracture pattern reflects the behavior of the main fault with a reverse dip-slip. Due to the clustering of fault-slip data (fig. 6d), standard inversion results (fig. 6d) were compared to the results of a "fixed" inversion developed for poorly distributed data sets [Bellier and Zoback, 1995], in which the principal stress axes are fixed to lie in the horizontal and vertical planes. The results are similar to the ones obtained from standard inversion, indicating that the results of figure 6d (i.e., N189°E-trending, horizontal σ_1), are significant and stable.

In summary, those results allow constraining a finite homogeneous stress state controlling reverse slip (horizontal σ_1 and σ_2) on the TRF, with a slight sinistral component along the eastern fault segment driven by NNE-trending compression.

PALEOGEOGRAPHIC AND MORPHOLOGICAL CONSTRAINTS ON THE EVOLUTION OF THE TRÉVARESSE RIDGE ANTICLINE

Neogene evolution

During the Neogene, Provence was shaped by the progressive southwestward propagation of the Miocene perialpine sea. This transgression proceeded in successive pulses, the coastlines going back and forth from the Burdigalian to the Tortonian, each of these pulses having generated regional-scale erosional planation surfaces on land and nonconformities within the Miocene basin [Aguilar and Clauzon, 1982 ; Champion *et al.*, 2000]. The 14-Ma-old Serravallian trangressive surface cuts Burdigalian marine sediments and Oligocene limestones of the western Trévaresse ridge at a very low angle [Aguilar and Clauzon, 1979]. The western Trévaresse ridge area, that corresponds to the southeasternmost extension of the Serravallian marine sediments, represents the southern margin of the Cucuron basin at that time [Aguilar and Clauzon, 1979] (fig. 1 and 7).

The 11 Ma old Tortonian transgression [Champion *et al.*, 2000] brought the coastline further to the south and

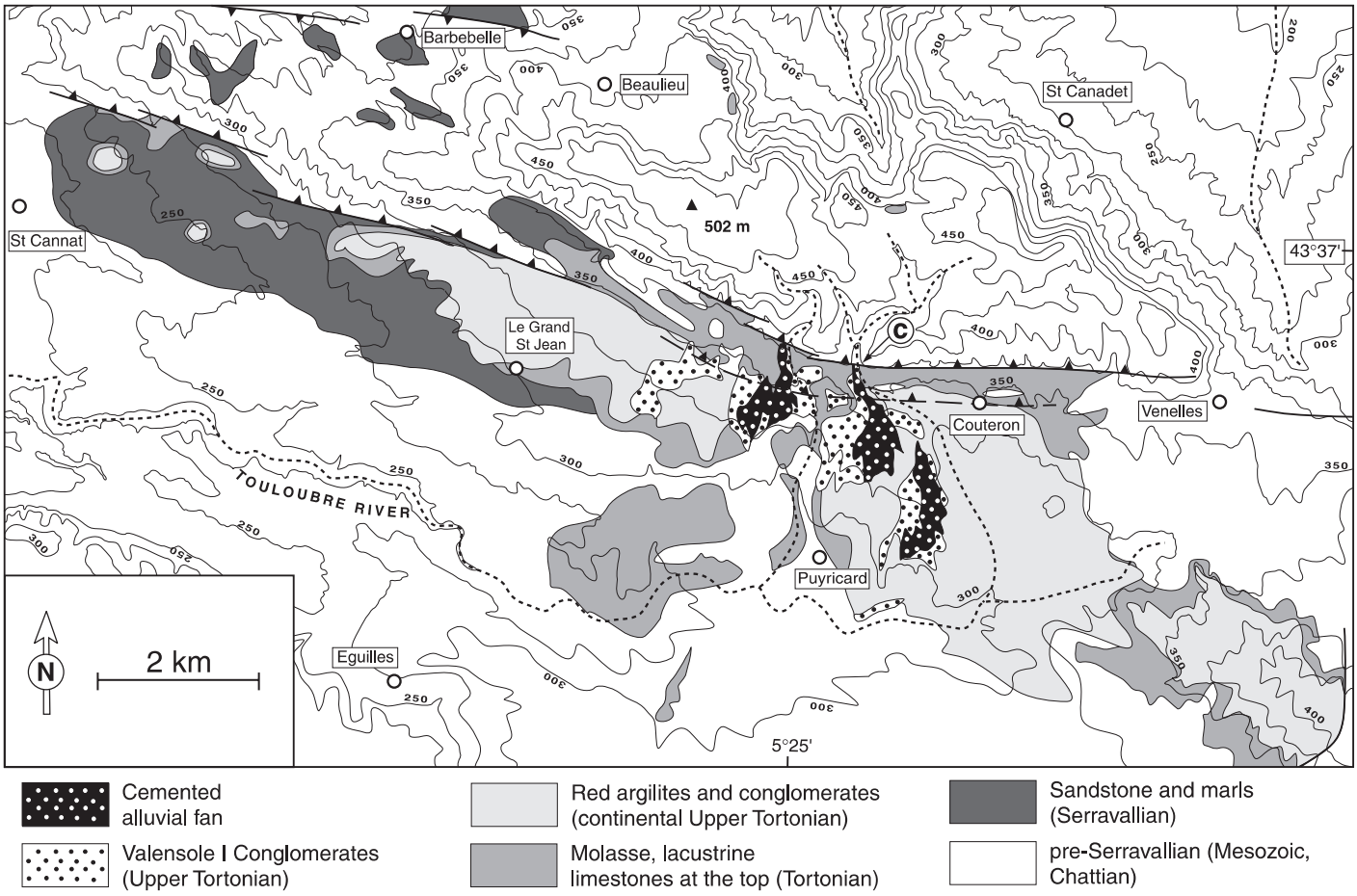

FIG. 7. – Topography and Neogene geology of the Trévaresse ridge anticline and Puyricard syncline. Geology is after Dubois [1964], Gouvernet *et al.* [1967, 1970], Aguilar and Clauzon [1979] and new field mapping. Elevation contours are 25 meters
FIG. 7. – *Topographie et géologie du Néogène de l'anticlinal de la Trévaresse et du synclinal de Puyricard. Géologie d'après Dubois [1964], Gouvernet* et al. *[1967, 1970], Aguilar et Clauzon [1979] et la présente étude. L'équidistance des courbes de niveau est de 25 m.*

east, up to the Aix-en-Provence area and the southern Sub-Alpine Chains front (fig. 1) and covered up the Trévaresse ridge area (fig. 7). The marine Tortonian formations lie unconformably on the Serravallian molasse in the Puyricard syncline and are locally preserved within the Trévaresse ridge (fig. 7). The flat topography around the top of the ridge may even correspond to a remnant of the Tortonian planation surface. In the eastern Trévaresse ridge, on both limbs of the anticline, this planation surface, characterized by conspicuous lithophage perforations, lies conformably, at least at the outcrop scale, on the Chattian limestone beds and the overlying Tortonian marine formations. This indicates that the amplification of the anticline, although probably initiated before the Tortonian [e.g., Aguilar and Clauzon, 1979], took place essentially after 11 Ma (i.e., after the development of the Tortonian planation surface).

The Puyricard syncline sediments represent the continental piedmont depositional sequence with respect to the ridge from Tortonian times to the present (fig. 5 and. 7). A Pontian (i.e., Messinian) age had previously been assigned to this sequence by Gouvernet *et al.* [1970]. However, a detailed biostratigraphic study of the laterally equivalent sequence in the Cucuron basin [Clauzon, 1981 ; Aguilar and Clauzon, 1982] (fig. 1) has revealed a late Tortonian age, allowing to assign the same age to the Puyricard piedmont basin.

The marine – continental transition associated with the last Miocene regression is dated at 8.5 Ma by rodent fauna at the longitude of the Trévaresse ridge [Aguilar and Clauzon, 1982]. The red argilites [Gouvernet *et al.*, 1970], unconformably overlying the Tortonian lacustrine limestones, represent the dominant facies of the piedmont sequence (fig. 5 and 7). Late Tortonian fluvial conglomerates of the Valensole I formation (fig. 7) are laterally equivalent to the argilites and are separated from the underlying marine and lacustrine strata by a channelling disconformity. Those conglomerates seem to be associated with a paleomeander of the Touloubre River. The red beds are not observed north of the Couteron anticline (fig. 5 and 7). This suggests denudation consecutive to uplift of the Couteron anticline (possibly together with the Trévaresse ridge anticline) above the Couteron blind reverse fault that must have taken place after the deposition of the Valensole I conglomerates. Indeed, the conglomerates appear to be affected by the Couteron anticline in the stream cut 1 km west of station (c) (fig. 7). These observations could suggest that the TRF and Trévaresse ridge anticline became locked by the end of the deposition of the Valensole I conglomerates, leading to the nucleation and southward propagation of the Couteron blind reverse fault after 5.8 Ma (i.e., the minimum age of the Valensole I formation).

Mechanical erosion products of the Trévaresse ridge anticline are found in the piedmont sequence as conglomerates cemented by the red argilites (fig. 7). The pebbles are angular and almost exclusively made of Chattian Limestones and flint nodules from the Trévaresse ridge anticline. Those deposits are also lateral equivalents to the Valensole I fluvial conglomerate [Gouvernet *et al.*, 1970]. This is particularly exemplified at station c (fig. 5 and 7), where the meander lies close to the TRF. There, the cm-scale, rounded fluvial pebbles of the Valensole I formation are mixed with pluridecimetric– to metric-scale angular blocks of Chattian limestone (fig. 5b), indicating active scarp degradation along the TRF during late Tortonian fluvial sedimentation (i.e., after 8.5 Ma, the age of the marine – continental transition, and before 5.8 Ma, the lower age limit for the Valensole I formation [Clauzon, 1996]). Furthermore, the fact that conspicuous mechanical striae were measured on the angular blocks at this location (fig. 5b and 6c) indicates that the upper piedmont of the Trévaresse ridge was still undergoing shortening after 5.8 Ma.

Quaternary evolution and qualitative geomorphology

The most prominent Quaternary piedmont formations seen in the Puyricard syncline are attributed to the Rissian (300 to 100 ka old) by Gouvernet *et al.* [1970]. These are remnants of two alluvial fans whose abandonment surface is still seen in the present topography, due to calcrete-type duricrusting (fig. 5 and 7). The fans are essentially made of Chattian limestone and flint debris coming from the Trévaresse ridge and a few reworked pebbles of the Valensole I formation. Their apexes coincide with the outlet of two streams that contributed to regressive incision of the anticline (fig. 7). Direct field observations do not allow determining whether the fans are faulted or whether they seal the TRF (fig. 5). Thanks to a recent roadside cut, we found a remnant of the fan with its characteristic weathering profile north of the TRF (fig. 5a). This outcrop seems to coincide with the northward extrapolation of the fan abandonment surface from the piedmont into the massif (fig. 5a). This observation does not yet allow evaluating whether reverse slipping took place along the TRF after the emplacement of the fan, but indicates that folding of the Trévaresse ridge and reverse displacement along the TRF were at least largely achieved at the time of fan development. The preservation of those fans, together with the microtectonic data at station c (fig. 5b and 6c), further shows that tectonic shortening and progradation of the Trévaresse ridge upper piedmont have still been active between 5.8 Ma and the late mid-Pleistocene. Indeed, it is during this time interval that southward migration of the Touloubre River course took place (between the Messinian abandonment of the Valensole I formation and the emplacement of the Rissian alluvial fans). The fact that the fans' abandonment surface is not apparently perturbed above the Couteron anticline (fig. 5a) at least suggests limited displacement along the Couteron blind reverse fault after the Rissian.

A topographic scarp systematically marks the TRF surface trace [Lacassin *et al.*, 2001] and underlines the lithologic contact between the Chattian limestones of the anticline and the Miocene formations (fig. 7). This is especially the case in the folded domain occupying the relay zone, where no fault is observed at the surface (fig. 7). This suggests, as pointed out by Mattauer [2002], that significant differential erosion took place at the forelimb of the Trévaresse ridge anticline and all along the TRF, due to a resistance contrast between the two lithologies, and that the scarp cannot be interpreted as a simple result of cumulative coseismic movements as suggested by Lacassin *et al.* [2001]. It is however interesting to note that along the eastern TRF segment, the fault scarp has undergone limited retreat (~ 400 m), and that the Tortonian surface envelop of the fold is only moderately dissected (fig. 7), indicating an overall youthful morphology of the structure. The eastern segment of the fault and its WNW trending folded termination arms the highest relief of the ridge (above 400 m-high), a crescent-shaped massif that parallels the bend of the segment (fig. 7 and 8). Along this segment, northward-directed regressive erosion of that massif has taken place, essentially

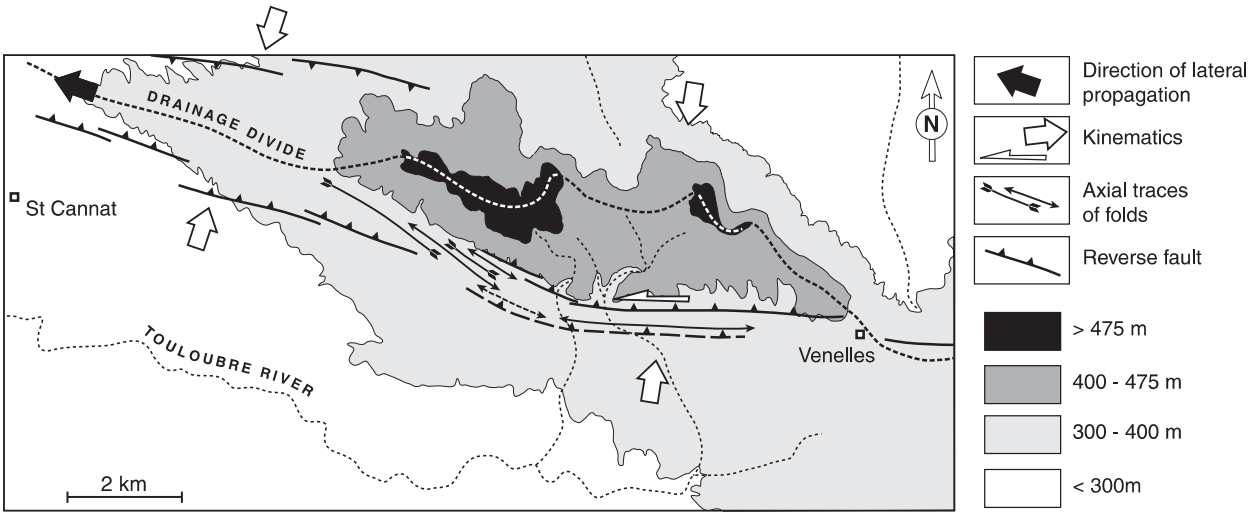

FIG. 8. – Sketch summarizing the relations between topography, structure and kinematics of the Trévaresse ridge anticline and the Trévaresse reverse fault.
FIG. 8. – *Schéma récapitulatif des relations entre topographie, structure et cinématique de l'anticlinal de la Trévaresse.*

before the Rissian (i.e., the age of the fans), starting from the main fault scarp (fig. 7). This resulted in a northward migration of the drainage divide of about 2 km with respect to the Trévaresse ridge anticline crest line (fig. 8).

By contrast, the western segment of the TRF flanks the low elevation (200 to 350-m-high), rectilinear, western termination of the anticline that plunges to the west (fig. 2 and 7). In this area, the relief associated with the anticline is not significantly dissected by erosion, suggesting an immature morphology of this segment of the anticline. The Trévaresse ridge drainage divide runs parallel to the fault segment trace at a short distance from the latter (less than 1 km far from the fault scarp, fig. 8).

To summarize, the two segments of the TRF and associated portions of the anticline have a distinctive geomorphic signature that suggests a diachronous morphotectonic evolution along the Trévaresse ridge. Indeed, geomorphic features indicate an early and higher amplification of the fold and a more mature erosional pattern along the eastern segment of the fault, and a later, less amplified portion of the fold with a rather immature morphological expression associated with the western segment of the fault. This points to the westward propagation of the Trévaresse ridge anticline [e.g. Keller *et al.*, 1999] associated with the sequential activation of the two segments of the TRF, this westward propagation being possibly related to the slight sinistral component of slip along the eastern TRF segment (fig. 8).

FAULT SLIP RATE

The offset of the Tortonian marine planation surface may be used to estimate the cumulative vertical displacement rate along the TRF over the past 11 Ma. Two hypotheses may be envisaged. The first one considers the present topography of the Trévaresse ridge as the partly dissected surface envelop of the folded Tortonian planation surface. Accordingly, the highest vertical displacement rate may be derived from the elevation difference between the top of the ridge (500 m) and the lowest elevation of the same surface in the Puyricard syncline (300 m). This leads to a displacement rate of 0.02 mm/yr. A more conservative hypothesis considers the elevation of the base of the Tortonian formations on the back limb of the anticline SE of St Canadet (425 m) as equivalent to the highest point of the surface envelop of the planation surface in the ridge (fig. 7). This leads to a vertical displacement rate of 0.01 mm/yr. Considering a minimum and maximum dip of 60 and 80° respectively for the TRF, the resulting average slip rate along the fault would be 0.03 ± 0.02 mm/yr.

This long-term estimate lies below the slip rate range of 0.05 to 0.2 mm/yr that characterizes individual strike-slip faults in Provence [e.g., Baroux, 2000 ; Hippolyte and Dumont, 2000 ; Schlupp *et al.*, 2001 ; Siame *et al.*, 2002]. However, this result may not be a totally accurate estimate of the active fault slip rate as it is an averaged value over the last 11 Ma that may integrate temporal variations in the slip rate on the fault over that period.

GEOMETRY OF THE FAULT AT DEPTH AND THE SOURCE OF THE LAMBESC EARTHQUAKE

Microseismic data analysis and seismogram processing of Baroux *et al.* [2001a ; 2002 ; 2003] lead to the following source parameters for the Lambesc earthquake. The rupture plane would trend N 110 E with a length of about 10 km for a width of about 6 km and a hypocenter depth of 1 to 6 km. Three configurations for the geometry of the TRF a depth may be tested in relation to both these parameters and the geological contraints (fig. 9).

In the case the TRF was connected to the Rognes anticline fault ramp (fig. 9a), a shallow hypocenter would be expected to be produced on a décollement layer at less than 1.5 km depth. Using the commonly accepted scaling laws between rupture area of faults and magnitudes [Wells and Coppersmith, 1994], this hypothesis would provide a rupture width that would be too small to produce a magnitude 6 earthquake.

The second possibility is that the TRF roots into a décollement layer in Upper Jurassic black shales that con-

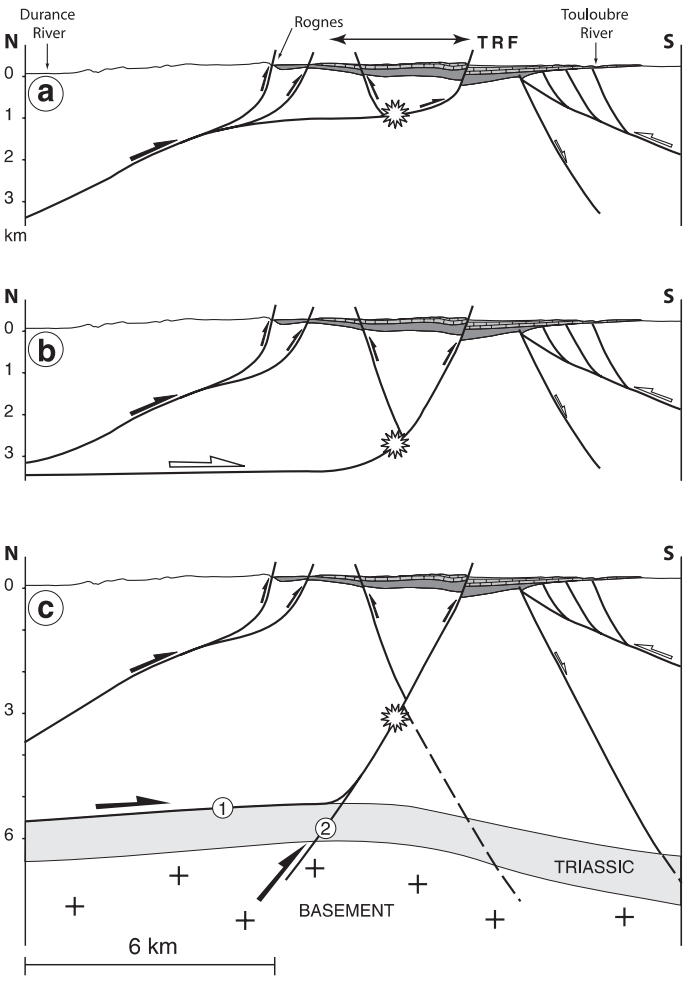

FIG. 9. – Hypotheses for the geometry of the Trévaresse Reverse Fault at depth in relation with the Lambesc earthquake hypocenter. The horizontal double arrow shows the location range of the epicenter of Baroux *et al.* [2002, and 2003].
FIG. 9. – *Hypothèses d'enracinement de la faille de la Trévaresse. La double flèche horizontale montre la gamme de localisation de l'épicentre d'après Baroux* et al. *[2002, and 2003].*

stitute the shallowest potential low strength layer in the Mesozoic series (fig. 9b). According to the scaling laws, this configuration would not allow a M = 6 earthquake to take place along the fault. Indeed, the area of the fault that ruptured was of about 60 km^2 [Baroux *et al.*, 2002, and 2003], whereas the maximum area that could rupture above the décollement is of 48 km^2, taking into account a total length of 14 km for the TRF.

The third hypothesis is that the fault reaches or cuts across the Triassic evaporitic layer at the base of the sedimentary pile (hypotheses 1 and 2, respectively, on fig. 9c). In that case, the area of the fault that could rupture (~ 100 km^2) exceeds the area necessary for producing a M = 6 earthquake [Wells and Coppersmith, 1994], considering that the 1909 earthquake reactivated the entire length of the TRF segments. In addition, this interpretation agrees with the evidence (see next paragraph) for possible early normal faulting along the TRF and the Beaulieu fault.

The 17.5 Ma old (Ar-Ar age, Aguilar *et al.* [1996]) Beaulieu basalts (fig. 2), are located at the eastern termination of the Beaulieu fault. Those basalts, containing numerous peridotite xenoliths, are contemporaneous with the last increments of the Oligocene to late early Miocene rifting episode that affected Provence and that subsequently led to the formation of the Ligurian – Provençal ocean basin [e.g., Cheval *et al.*, 1989]. On the back limb of the Trévaresse ridge anticline, a few tens of meters from the fold hinge, the Upper Chattian limestones and marls are affected by macroscale, north-dipping, syn-sedimentary normal faults. Some of these faults show evidence for positive inversion (i.e., they are reactivated as southerly-verging reverse faults, similar to the TRF). This suggests that the Beaulieu fault and the TRF were originally normal faults active during the late Oligocene and probably until the Burdigalian (17.5 Ma), that is in agreement with evidence for normal faulting of Burdigalian sediments in southern Provence [e.g., Hippolyte *et al.*, 1993]. The pop-up structure developed by those two faults as a result of late Neogene and possibly Quaternary shortening might therefore have been a late Paleogene graben, juxtaposed to the south to a horst bounded by the TRF and La Barben fault (fig. 3c and 9c). These three faults would be similar to the inverted Oligocene normal faults buried under the Cucuron basin [e.g., Roure *et al.*, 1992] (fig. 10).

To summarize, considering the constraints provided both by the Lambesc earthquake source parameters [Baroux *et al.*, 2003] and the surface geology, we favor the third hypothesis where the TRF crosscuts the entire Meso-Cenozoic sedimentary pile (fig. 9c). In that case, the Beaulieu fault and the TRF might even cut across the cover / basement boundary (fig. 9c), providing a sufficient area to produce a M=6 earthquake (fig. 10).

At a regional scale, the TRF occupies a specific structural setting in the western Provence panel (fig. 1), that can be divided into two units : (1) the quasi-rigid Plateau de Vaucluse unit, north of the Luberon ramp anticline and (2) the faulted unit underlying the Luberon anticline and the Cucuron basin and bounded to the south by the TRF (fig. 10). In the case this unit is decoupled from its basement along the Triassic evaporitic décollement layer as suggested on figure 10, the TRF would be connected to the southerly-verging Luberon basement thrust ramp [Roure and Colletta, 1996], and would be the frontal emerging thrust fault of a crustal-scale flat-and-ramp system. The Triassic décollement layer would transmit the stress accumulated across the Plateau de Vaucluse unit and against the Luberon basement thrust ramp. One should add that the topography of both the top and the base of the Luberon-Cucuron unit mimics the basement-cover interface that is controlled by two basement culminations [Tempier, 1987 ; Champion *et al.*, 2000]. The gravitational potential of the decoupled sedimentary pile would therefore play a first-order role in mechanically charging the TRF together with the compression acting along the two bounding faults of the Neogene western Provence thrust system (i.e., the Ventoux – Montagne de Lure and Trévaresse).

DISCUSSION AND CONCLUSION

Seismological and macroseismic data indicate that the Lambesc earthquake took place along a fault bounding the Trévaresse ridge to the south. The present study confirms and further documents the presence at the surface of this steeply north-dipping reverse fault, the TRF, affecting the

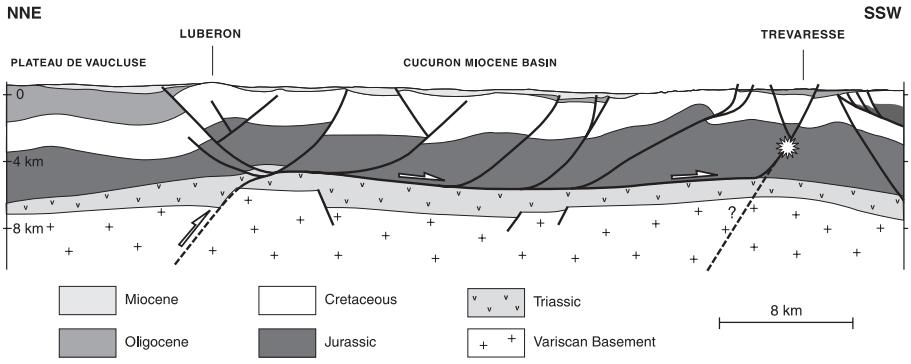

FIG. 10. – Cross-section of the western Provence panel. Possible hypocenter of the Lambesc earthquake is shown. The northern part of the section is adapted from reflection seismics interpretations of Champion *et al.* [2000] and a balanced cross-section of Roure and Colletta [1996]. Basement-cover boundary is based on Menard [1980]. Location on figure 1.

FIG. 10. – *Coupe du panneau ouest provençal. Un hypocentre possible pour le séisme de Lambesc est représenté. La partie nord de la coupe est basée sur des interprétations de sismique pétrolière [Champion* et al.*, 2000] et une coupe équilibrée de Roure et Colletta [1996]. La profondeur du socle est adapté de Ménard [1980]. Localisation sur la figure 1.*

forelimb of the Trévaresse ridge anticline. The fold-fault relationships could suggest that the TRF is a "steep-limb breakthrough thrust" [Suppe and Medwedeff, 1990], i.e., a late-stage, steep reverse fault that nucleates from the main blind ramp and propagates upward to cut across the forelimb of a fault-propagation anticline [Mercier *et al.*, 1997]. As the TRF appears to be an inverted normal fault that did exist at the onset of shortening, the anticline is therefore not appropriately described by a fault-propagation fold kinematic model. The fold should therefore be considered as a forced ramp anticline developed above the TRF that roots into the Triassic décollement layer or may even crosscut the basement-cover interface at a minimum depth of 6 km.

Folding and thrusting of the Trévaresse ridge anticline took place essentially during late Miocene and Pliocene times and possibly after the mid-Pleistocene. Over the last 11 Ma, the TRF records cumulative reverse slip with a minor sinistral component related to NNE-trending compression and a long-term slip rate of 0.03 ± 0.02 mm/yr. The fault is segmented into two major segments separated by a transpressive relay zone affected by an en-échelon fold pattern. This fold pattern is compatible with the sinistral strike-slip component of the eastern segment and may have recorded the westward propagation of the TRF and Trévaresse ridge anticline. A post early Pliocene frontal fault-propagation fold developed above a blind reverse fault linked to the eastern TRF segment. This blind fault may be connected to the western emerging segment of the fault across the gap.

First order qualitative geomorphic observations suggest a westward propagation of the fold during partly diachronous activation of the two segments of the TRF. Although our results do not preclude post-early Pleistocene slip along the TRF system, the fault scarp is not unequivocally interpreted as resulting from cumulative late Quaternary coseismic displacements along the fault. Paleoseismological, geophysical [e.g., Nguyen *et al.*, 2002] and quantitative geomorphology studies in progress aim at revealing the Quaternary activity of the emerging and blind segments of the TRF.

Given its specific structure and evolution, the Trévaresse ridge anticline may not be readily compared with emerging fault-related folds developed in rapidly deforming regions such as Central Asia [e.g., Tapponnier *et al.*, 1990]. Rather, it shares several similarities with, for instance, the active coastal folds of the south Atlas front of Morocco (e.g., short, steep to overturned forelimb, steep to vertical emerging faults) that also developed in a context of low- to moderate seismicity and slow deformation [Meghraoui *et al.*, 1998]. In such seismotectonic contexts, a strong and complex structural inheritance is expected to control the development of active ramp anticlines, requiring a detailed knowledge of the structure and long-term morphotectonic evolution of the folds to target high-resolution active deformation studies and ultimately addressing seismic hazard assessment.

Acknowledgment. – An excursion led by P. Choukroune in 1996 along the Trévaresse reverse fault allowed addressing the potentially coseismic origin of some geomorphic features of the fault scarp (especially the scarplet discussed by Lacassin *et al.* [2001]) and was the starting point for the current studies on the Trévaresse ridge anticline. Our research on the Lambesc earthquake is funded by the Action Concertée Incitative "Prévention des Catastrophes Naturelles" and the E.U. S.A.F.E. project (EVG1-2000-22005). We are indebted to P. Choukroune, G. Clauzon and M. Sébrier for fruitful discussions and suggestions and to F. Garcia, J. Juilleret and B. Laugier for their collaboration at various stages of this study. We thank J.-C. Hippolyte, and N. D'Agostino for their constructive reviews of an earlier version of the manuscript and D. Frizon de Lamotte for editorial suggestions. SPOT images ((c) CNES) were provided by the ISIS program. Processing of topographic and satellite image data were performed at the CEREGE STSI facility with the help of Ph. Dussoulliez and B. Simon.

References

AGUILAR J.-P. & CLAUZON G. (1979). – Un gisement à mammifères dans la formation lacustre d'âge miocène moyen du Collet Redon près de St-Cannat (Bouches du Rhône). Implications stratigraphiques. – *Palaeovertebrata*, **8**, 327-341.

AGUILAR J.-P. & CLAUZON G. (1982). – Evolution géodynamique de la Provence septentrionale au cours du Miocène supérieur et terminal d'après les faunes de rongeurs. – *C. R. Acad. Sci.,* Paris, **294**, 915-920.

AGUILAR J.-P., CLAUZON G., DE GOËR DE HERVÉ A., MALUSKI H., MICHAUX J. & WELCOMME J.-L. (1996). – The MN3 fossil mammal-bearing locality of Beaulieu (France) : biochronology, radiometric dating, and lower age limit of the early Neogene renewal of the mammalian fauna in Europe. – *Newsl. Stratigr.*, **34**, 177-191.

AVOUAC J.P. *et al.* (1993). – p. 23.

AVOUAC J.P., TAPPONNIER P., BAI M., YOU H. & WANG G. (1990). – Active thrusting and folding along the northern Tien Shan and late Cenozoic rotation of the Tarim relative to Dzungaria and Kazakhstan. – *J. Geophys. Res.,* **98**, 6755-6804.

BAROUX E. (2000). – Tectonique active en région à sismicité modérée : le cas de la Provence (France), Apport d'une approche multidisciplinaire. – Thèse, Université Paris Sud, Orsay, 327 p.

BAROUX E., VALENSISE G., PINO N.A., SCOTTI O., CUSHING M. & BELLIER O. (2001a). – Modeling the 1909 Lambesc earthquake with geodetic, macroseismic and instrumental data : implication for seismic hazard in Provence (France). – Abstract, *26th E.G.S. assembly, Nice.*

BAROUX E., BÉTHOUX N. & BELLIER O. (2001b). – Analyses of the stress field in southeastern France from earthquake focal mechanisms. – *Geophys. J. Int.*, **145**, 336-348.

BAROUX E., PINO N.A., VALENSISE G., SCOTTI O. & CUSHING M. (2002). – Source mechanism of the 11th June 1909 Lambesc (Provence, France) earthquake from macroseismic, seismological and geodetic data : constraints for active tectonic deformation in Southeastern France. – Abstract, *27th E.G.S. assembly, Nice.*

BAROUX E., PINO N.A., VALENSISE G., SCOTTI O. & CUSHING M. (2003). – Source parameters of the 11 June 1909, Lambesc (southern France) earthquake : a reappraisal based on macroseismic, seismological and geodetic observations. – *J. Geophys. Res.* (in press).

BELLIER O. & ZOBACK M.L. (1995). – Recent state of stress change in the Walker Lane zone, western Basin and Range province, United States. – *Tectonics*, **14**, 564-593.

BUSSER T. & PACHOUD A. (1966). – Contribution à l'étude géologique des chaînons compris entre l'Arc et la vallée de Lambesc à l'ouest d'Aix-en-Provence. – *Bull. Soc. géol. Fr.,* **(7) VIII**, 786-792.

CALAIS E., NOCQUET J.-M., JOUANNE F. & TARDY M. (2002). – Current strain regime in the western Alps from continuous Global Positioning System measurements, 1996-2001. – *Geology*, **30**, 651-654.

CARBON D. (1996). – Pré-étude des indices de déformation récente des chaînons provençaux. – Rap. GTR/CEA/1096-60. (Dépôt IRSN).

CAREY E. (1979). – Recherche des directions principales de contraintes associées au jeu d'une population de failles. – *Rev. Géol. Dyn. Géogr. Phys.*, **21**, 57-66.

CHAMPION C., CHOUKROUNE P. & CLAUZON G. (2000). – La déformation post-miocène en Provence occidentale. – *Geodin. Acta*, **13**, 67-95.

CHEVAL F., DAUTRIA J.-M. & GIROD M. (1989). – Les enclaves de lherzolite à grenat et spinelle du volcan burdigalien de Beaulieu (Bouches-du-Rhône) : des témoins d'une remontée du manteau supérieur associée à l'ouverture du bassin océanique provençal. – *C. R. Acad. Sci.,* Paris, **309**, 1309-1315.

CLAUZON G. (1981). – Révision du stratotype du Pontien méditerranéen (Deperet, 1893) et relations de cet étage continental avec l'évolution géodynamique de la marge méditerranéenne française au Miocène supérieur. – *C.R. Acad. Sci*., Paris, **293**, 309-314.

CLAUZON G. (1996). – Limites de séquences et évolutions géodynamiques. – *Géomorphologie*, **1**, 3-22.

CLAUZON G. & ROBERT C. (1984). – La sédimentation argileuse du Miocène supérieur continental dans le bassin de Cucuron/basse Durance (Provence, France) : implications paléogéographiques. – *Paléobiol. Continent.*, **14**, 205-224.

COMBES P. (1984). – La tectonique récente de la Provence occidentale : microtectonique, caractéristiques dynamiques et cinématiques. Méthodologie de la zonation tectonique et relations avec la sismicité. – Thèse, Université Louis Pasteur, Strasbourg, 182 p.

COMBES P., CARBON D., CUSHING M., GRANIER T. & VASKOU P. (1993). – Mise en évidence d'un paléoséisme pléistocène supérieur dans la vallée du Rhône : implications sur les connaissances de la sismicité en France. – *C.R. Acad. Sci.,* Paris, **317**, 689-696.

DEMETS C., GORDON R.G., ARGUS D.F. & STEIN S. (1990). – Current plate motions. – *Geophys. J. Int.*, **101**, 425-478.

DUBOIS P. (1964). – Reconnaissance stratigraphique et tectonique du Miocène de la Provence occidentale. – Rap. Comp. Explor. Pétrol., Marseille, 42 p. (Dépôt CEREGE).

DUBOIS P. (1966). – Sur la sédimentation et la tectonique du Miocène de la Provence occidentale. – *Bull. Soc. géol. Fr.*, **(7) VIII**, 793-801.

DUTOUR A., PHILIP H., JAURAND E. & COMBES P. (2002). – Mise en évidence de déformations en faille inverse avec ruptures de surface cosismiques dans les dépôts würmiens du versant nord du mont Ventoux (Provence Occidentale, France). – *C. R. Géoscience*, **334**, 849-856.

FERHAT G., FEIGL K., RITZ J.-F. & SOURIAU A. (1998). – Geodetic measurement of tectonic deformation in the southern Alps and Provence, France. – *Earth Planet. Sci. Lett.*, **159**, 35-46.

GABERT J. (1965). – Phénomènes périglaciaires du Quaternaire supérieur et néotectonique dans la région de l'Etang de Berre (basse Provence occidentale). – *90ème Cong. Soc. Sav., Nice*, **II**, 75-88.

GOUVERNET C. (1963). – Le Miocène de la Région de Salon-de-Provence. Stratigraphie et tectonique. – *Ann. Fac. Sci. Marseille*, **43**, 129-145.

GOUVERNET C., GUEIRARD S., CATZIGRAS F., DURAND J.-P., GUIEU G., GERVAIS J., PHILIP J., ROUSSET C., TEMPIER C., ARLHAC P., BLANC J.-P., GRÉGOIRE J.-Y., LAMBERT C., CHATUÉ-KAMGA, VINCENT H. & ROUIRE J. (1967). – Carte géologique de la France, 1/80 000, Aix. – Ministère de l'Industrie, Paris.

GOUVERNET C., COLOMB E., GERVAIS J., GUEIRARD S., NURY D. & ROUIRE J. (1968). – Carte géologique de la France à 1/50 000, Salon de Provence (XXXI-43). – BRGM, Orléans.

GOUVERNET C., ROUIRE J. & ROUSSET C. (1970). – Carte géologique de la France à 1/50 000, Pertuis (XXXII-43). – BRGM, Orléans.

GUIEU G. & ROUSSET C. (1978). – Structures, paléostructures, paléogéographie et genèse des bauxites en Provence. – *Bull. BRGM*, **(2) II**, 311-322.

HIPPOLYTE J.-C., ANGELIER J., BERGERAT F., NURY D. & GUIEU G. (1993). – Tectonic-stratigraphic record of paleostress time changes in the Oligocene basins of the Provence, southern France. – *Tectonophysics*, **226**, 15-35.

HIPPOLYTE J.-C. & DUMONT T. (2000). – Identification of Quaternary thrusts, folds and faults in a low seismicity area : examples in the southern Alps (France). – *Terra Nova*, **12**, 156-162.

JOUANNE F., HIPPOLYTE J.-C., GAMOND J.-F. & MARTINOD J. (2001). – Current deformation of the Digne Nappe (southwestern Alps) from a comparison between triangulation and GPS data. – *Geophys. J. Int.*, **144**, 432-440.

KELLER E.A., GURROLA L. & TIERNEY T.E. (1999). – Geomorphic criteria to determine the direction of lateral propagation of reverse faulting and folding. – *Geology*, **27**, 515-518.

LACASSIN R., TAPPONNIER P., MEYER B. & ARMIJO R. (2001). – Was the Trévaresse Thrust the source of the 1909 Lambesc (Provence, France) earthquake ? Historical and geomorphic evidence. – *C.R. Acad. Sci.,* Paris, **333**, 571-581.

LACASSIN R., TAPPONNIER P., MEYER B. & ARMIJO R. (2002). – Réponse au commentaire de Maurice Mattauer à l'article : Was the Trévaresse Thrust the source of the 1909 Lambesc (Provence, France) earthquake ? Historical and geomorphic evidence. – *C.R. Géoscience,* **334**, 515-517.

LALLEMAND C. (1911). – Sur les changements de niveau du sol en Provence. – *C. R. Acad. Sci.,* Paris, **152**, 1560-1562.

LAMBERT J. *(Editeur)*, (1997). – Les tremblements de terre en France. – Editions BRGM, Orléans, 196 p.

LEVRET A., CUSHING M. & PEYRIDIEU G. (1996). – Etude des caractéristiques de séismes historiques en France. Institut de Protection et de Sûreté Nucléaire, 399 p.

LEVRET A., LOUP C. & GOULA X. (1986). – The Provence earthquake of 11th June 1909 (France). A new assessment of near field effects. – Extended abstract, *8th European Conference on earthquake engineering*, *Lisbonne*.

MATTAUER M. (2002). – Commentaire à la publication de Robin Lacassin *et al.* intitulée : Was the Trévaresse thrust the source of the 1909 Lambesc (Provence, France) earthquake ? Historical and geomorphic evidence. – *C.R. Géoscience,* **334**, 513-514.

MEGHRAOUI M., OUTTANI F., CHOUKKRI A. & FRIZON DE LAMOTTE D. (1998). – Coastal tectonics across the south Atlas thrust front and the Agadir active zone, Morocco. *In :* I.S. STEWART, and C. VITA-FINZI, Ed. Coastal tectonics. – *Geol. Soc. Spec. Publ.*, **146**, 239-253.

MÉNARD G. (1980). – Profondeur du socle antétriasique dans le Sud-Est de la France. – *C.R. Acad. Sci.,* Paris, **290**, 299-302.

MERCIER E., OUTTANI F. & FRIZON DE LAMOTTE D. (1997). – Late-stage evolution of fault-propagation folds : principles and example. – *J. Struct. Geol.*, **19**, 185-1997.

MERCIER J.-L., CAREY-GAILHARDIS E. & SÉBRIER M. (1991). – Paleostress determinations from fault kinematics : application to the neotectonics of the Himalayas-Tibet and Central Andes. – *Phil. Trans. Geol. Soc. Lond.*, **337**, 41-52.

NGUYEN F., GARAMBOIS S., CHARDON D., JONGMANS D., BELLIER O. & HERMITTE D. (2002). – Etude de failles actives par méthodes géophysiques combinées : exemple de la Trévaresse. – Résumé étendu, *Journées AGAP*, Nantes.

NURY D. (1990). – L'Oligocène de Provence méridionale. – *Doc. BRGM*, **163**, 1-418.

PEULVAST J.-P., BAROUX E., BELLIER O. & SÉBRIER M. (1999). – Le problème de l'activité des failles de Nîmes, Salon-Cavaillon et de la Moyenne Durance (SE de la France) : apports de la géomorphologie structurale. – *Géomorphologie*, **4**, 327-358.

PROVANSAL M., QUINIF Y., VERRECCHIA E. & ARNAUD P.M. (1995). – Identification d'un littoral tyrrhénien en bordure de l'Etang de Berre (Bouches-du-Rhônes, France méridionale). – *C.R. Acad. Sci.,* Paris, **320**, 867-872.

RITZ J.-F. (1991). – Evolution des champs de contraintes dans les Alpes du Sud depuis la fin de l'Oligocène. Implications sismotectoniques. – Thèse, Université Montpellier 2, Montpellier, 187 p.

ROMIEU C., MÉNARD G. & MOINE S. (1998). – Réévaluation des mouvements verticaux associés au séisme de Lambesc (Provence, 11 juin 1909). – *Mouvements actuels de la surface terrestre et des massifs rocheux : mesure et interprétation*, École d'été, Les Houches, 52-53.

ROURE F., BRUN J.-P., COLLETTA B. & VAN DEN DRIESSCHE J. (1992). – Geometry and kinematics of extensional structures in the Alpine

foreland basin of southeastern France. – *J. Struct. Geol.*, **14**, 503-519.

ROURE F. & COLLETTA B. (1996). – Cenozoic inversion structures in the foreland of the Pyrenees and Alps. *In* : P.A. ZIEGLER and F. HORVARTH Ed. Structure and prospects of Alpine basins and forelands. – *Peri-Téthys Mem.*, **2**, Paris ; MNHN Ed., 173-209.

SCHLUPP A., CLAUZON G. & AVOUAC J.-P. (2001). – Mouvement post-messinien sur la faille de Nîmes : implications pour la sismotectonique de la Provence. – *Bull. Soc. géol. Fr.,* **172**, 697-711.

SÉBRIER M., GHAFIRI A. & BLES J.-L. (1997). – Paleosismicity in France : Fault trench studies in a region of moderate seismicity. – *J. Geodyn.*, **24**, 207-217.

SIAME L., BELLIER O., SÉBRIER M., BOURLÈS D., BRAUCHER R., BAROUX E., BEAUDOUIN T., CUHING M., WINTER R., RAISBECK G.M. & YIOU F. (2002). – ^{10}Be down concentration profiles and high denudation rates : diagnostic criteria for identifying active deformation. – Abstract, *Goldsmith Conference*, Davos.

SPIESS (COMMANDANT SPIESS) (1926). – Note sur le tremblement de Terre de Provence du 11 juin 1909. – *Congrès des sociétés savantes*, Clermont-Ferrand.

SUPPE J. & MEDWEDEFF D.A. (1990). – Geometry and kinematics of fault-propagation folding. – *Eclogae Geol. Helv.*, **83**, 409-454.

TAPPONNIER P., MEYER B., AVOUAC J.P., PELTZER G., GAUDEMER Y., GUO SHUNMIN, XIANG HONGFA, YIN KELUN, CHEN ZHITAI, CAI SHUAHUA & DAI HUAGANG (1990). – Active thrusting and folding in the Qilian Shan, and decoupling between upper crust and mantle in northeastern Tibet. – *Earth. Planet. Sci. Lett.,* **97**, 382-403.

TEMPIER C. (1987). – Modèle nouveau de mise en place des structures provençales. – *Bull. Soc. géol. Fr.*, **8**, 533-540.

TERRIER M. (1991). – Néotectonique de la Provence occidentale (France) : vers une analyse multicritères des déformations récentes. Application à la classification des structures sismogènes. – *Mém. BRGM*, **207**, 1-232.

VELLA C. & PROVANSAL M. (2000). – Relative sea-level rise and neotectonic events during the last 6500 yr on the southern eastern Rhône delta, France. – *Mar. Geol.*, **170**, 27-39.

VILLEGER M. & ANDRIEUX J. (1987). – Phases tectoniques post-éocènes et structuration polyphasée du panneau de couverture nord provençal (Alpes externes méridionales). – *Bull. Soc. géol. Fr.*, (8) **III**, 147-156.

VOLANT P., BERGE-THIERRY C., DERVIN P., CUSHING M., MOHAMMADIOUN M. & MATHIEU F. (2000). – The southeastern Durance fault permanent network : preliminary results. – *J. Seismology*, **4**, 175-189.

WELLS D.L. & COPPERSMITH J. (1994). – New empirical relationships among magnitude, rupture length, rupture width, rupture area, and surface displacement. – *Seism. Soc. Am. Bull.*, **84**, 974-1002.